ISBN: 978-3-95450-216-5 doi:10.18429/JACoW-eeFACT2018-TUPBB05

BEAM INSTRUMENTATION AT SUPERKEKB

G. Mitsuka*, M. Arinaga, J. W. Flanagan, H. Fukuma, H. Ikeda, H. Ishii,
S. Iwabuchi, K. Mori, E. Mulyani, M. Tejima, and M. Tobiyama,
KEK Accelerator Laboratory, 1-1 Oho, Tsukuba 305-0801, Japan
also at Graduate School for Advanced Study (SOKENDAI), 1-1 Oho, Tsukuba 305-0801, Japan
G. S. Varner, U. Hawaii, Dept. Physics and Astronomy, 2505 Correa Rd., Honolulu HI 96822, USA
G. Bonvicini, Wayne State U., 135 Physics Bldg., Detroit MI 48201, USA

Abstract

Phase 2 commissioning of the SuperKEKB electron–positron collider has been performed with final focus optics from February 8 to July 17, 2018. The main aims of Phase 2 commissioning were to verify the novel nano-beam collision scheme and achieve the machine luminosity $O(10^{34}\,\mathrm{cm}^{-2}\mathrm{s}^{-1})$. The beam instruments including the bunch-by-bunch feedback and orbit feedback systems, which are central to the beam diagnostics at SuperKEKB, were successfully operated throughout Phase 2. In this talk, we will present the commissioning results focusing on beam diagnostics and show prospects for the final phase of commissioning from next spring.

INTRODUCTION

The SuperKEKB collider (2016–) is a major upgrade to the KEKB collider (1998–2010) at KEK. Colliding 7 GeV electrons in the high energy ring (HER) and 4 GeV positrons in the low energy ring (LER), with a factor of two higher beam currents and the novel nano-beam scheme [1], will provide 40 times larger luminosity than KEKB.

Commissioning of SuperKEKB has been proceeded along the following three periods. *Phase 1* from February 1 to June 28, 2016 aimed to perform scrubbing run for new vacuum chambers and low emittance tuning for new arc lattice. After closing Phase 1, the superconducting final quadrupoles (QCS) and the Belle II detector except for the inner silicon-based VXD tracking system were installed. *Phase 2* started on February 8, 2018 with commissioning of the positron damping ring (DR) and was followed by commissioning of the HER and LER from March 19 to July 17 , 2018. The main parameters of the HER, LER, and DR at Phase 2 are summarized in Table 1. *Phase 3* physics operation is scheduled from March 2019 with the complete Belle II detector.

Main tasks of Phase 2 are first to achieve electron–positron collisions, second to verify the nano-beam collision scheme, and finally to establish control of beam-induced backgrounds resulting from low beta functions at the interaction point (IP).

Beam instruments at SuperKEKB are designed for beam diagnostics, e.g. establishing the circulating orbit, finding the beam-beam kick, accumulating large beam currents, etc. In the rest of this paper, we present the performance of beam instrumentation at Phase 2 and prospects for Phase 3.

* gaku.mitsuka@kek.jp

BEAM INSTRUMENTATION AT DR

Beam Position Monitor

There are totally 83 beam position monitors (BPMs) in the DR [2]. A BPM consists of four button electrodes with a diameter of 6 mm, where two electrodes are attached each other in one flange (see Fig. 1). We use the detection circuit VME 18K11 L/R that employs a log-ratio amplifier.

Figure 2 shows a schematic diagram of the BPM timing system. First, the main frequency divider generates bunch revolution timing that is synchronized with the injection bunch timing. Second, the 32 channel digital delay unit inserted between the main frequency divider and 18K11 further adjusts the timing offset. The second timing adjustment is needed for the timing differences ~ 200 ns owing to the BPM locations relative to the injection point and sizable cable lengths.

Table 1: Main parameters of the SuperKEKB HER, LER, and DR at Phase 2

	HER	LER	DR
Energy (GeV)	7	4	1.1
Circumference (m)	3016		135
Max. current (mA)	800	860	12
Bunch length (mm)	5	6	6.6
RF frequency (MHz)	508.877		
Harmonic number	5120		230
Betatron tune (H/V)	44.54/ 46.56	45.54/ 43.56	8.24/ 7.17
Synchrotron tune	0.02	0.018	0.025
T. rad. damp time (ms)	58	43	12
x-y coupling (%)	0.27	0.28	10
Emittance (nm)	3.2	4.6	29
Peak luminosity ($\mathrm{cm}^{-2}\mathrm{s}^{-1}$)	5.5×10^{33}		
Beam position monitor	486	444	83
Turn-by-turn monitor	69	70	83
Trans. FB system	2	2	1
Visible SR monitor	1	1	1
X-ray size monitor	1	1	0
Betatron tune monitor	1	1	1
DCCT	1	1	1
Bunch current monitor	1	1	1
Beam loss monitor	105 (IC) and 101 (PIN)		34

ISBN: 978-3-95450-216-5 doi:10.18429/JACoW-eeFACT2018-TUPBB05

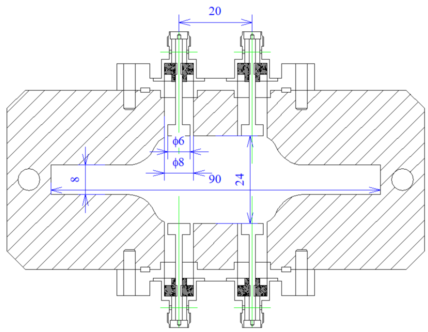

Figure 1: Cross section of the DR BPM.

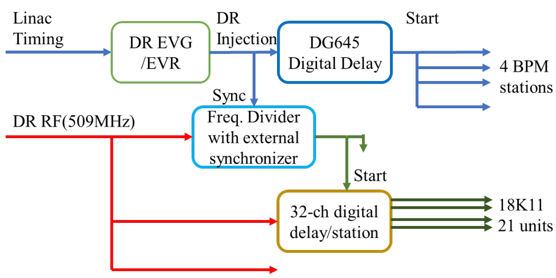

Figure 2: Block diagram of the DR BPM timing system.

The BPM block positions relative to the quadrupole magnets were surveyed using FARO 3D-ARM. The mean and 1σ standard deviation values for horizontal and vertical directions are (0.07 ± 0.47) mm and (-0.25 ± 0.29) mm, respectively. Gain difference among four electrodes was estimated as $< 8\,\%$ by the beam-based gain mapping method. The mean position resolution of the BPM system, 2–10 µm (horizontal) and 2–3 µm (vertical), was obtained using the 3-BPM method with 2k sample for 1 nC/bunch (see Fig. 3).

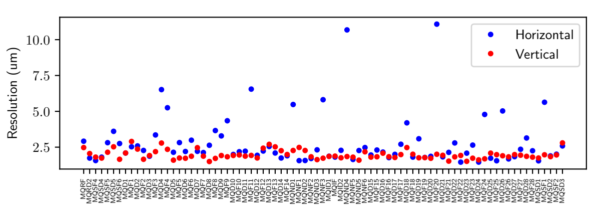

Figure 3: Position determination resolution of the DR BPMs.

Beam Size Monitors

Longitudinal and transverse beam sizes from injection to extraction were measured by a streak camera and a fast gated camera. Figure 4 shows examples of measured bunch lengths after the injection.

Beam Loss Monitors

Totally 34 ion chambers are installed along the DR and two beam transport lines. These monitors are sensitive to possible beam losses and inhibit the injection in case the loss exceeding the pre-defined threshold. We use the fast sample ADCs with digital peak hold circuit to monitor the integrated loss within 1 second.

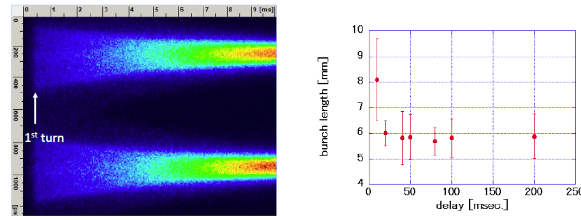

Figure 4: Measured bunch lengths in the DR after injection.

BEAM INSTRUMENTATION AT MAIN RINGS

Gated Turn-by-turn Monitor

The gated turn-by-turn monitor (GTBT, Fig. 5) is developed mainly for measurements of beam optics using a non-colliding bunch and injection beam orbit [3]. Four independent channels are each connected to a fast RF switch, a log-ratio beam signal detector, and a 14-bit ADC.

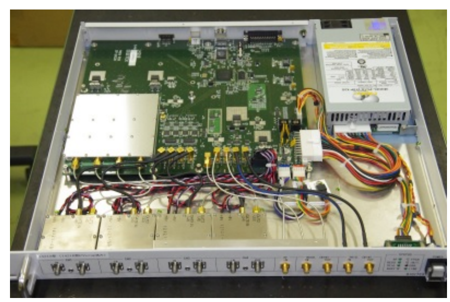

Figure 5: Photo of the gated turn-by-turn detector.

At SuperKEKB, optical functions such as betatron functions, x-y couplings and dispersions are usually measured by narrow-band BPMs using single kick method. Additionally, the GTBTs serve for measurements of the phase advances between the GTBTs. It is advantageous particularly around at the IP where the BPM gain and the BPM position relative to the QCS location are rather unreliable owing to fairly complex mechanical structure and large gain loss of the coaxial cables.

In the early stage of Phase 2, the GTBTs started the operation with the signal timing gate fully opened and successfully detected the injection beam orbit. Additional 19 GTBTs since Phase 2, located mainly around at the HER injection points and at the IP, contributed to smooth beam circulations. After beam storage we finely adjusted the ADC and gate timing. Note that the beam timing (definition of the bucket 0) was shifted wildly from Phase 1 mainly due to the insertion of the DR in the injection timing path.

Towards Phase 3, we plan to develop data processing software in the GTBTs' EPICS IOCs, such as a fast Fourier transform, correction for one-turn delay, etc. It enables quick optics measurements and GTBT data analyses in situ.

ISBN: 978-3-95450-216-5
doi:10.18429/JACoW-eeFACT2018-TUPBB05

Photon Monitors

X-ray monitors (XRMs) are installed one to each main ring primary for vertical beam size measurements [4]. Since the silicon pixel detectors and the fast readout systems developed under the US-Japan collaboration were not in time, we instead measured the vertical beam sizes by analyzing the X-ray-induced images projected on the scintillator screens (Fig. 6).

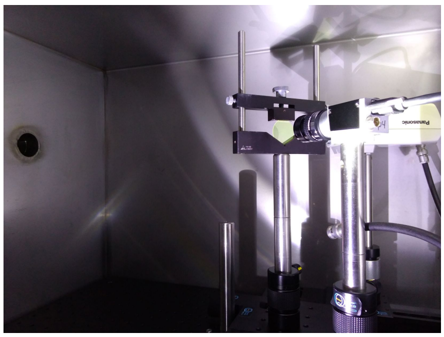

Figure 6: CCD camera and scintillator screen inside the XRM detector box.

At Phase 1 the LER XRM results on the vertical emittance (ε_y) agreed well with the optics estimation. However, in the HER, the XRM data gave 3.5 times larger ε_y compared with the optics estimation. The large ε_y might be caused by smearing effects ~ 32 µm remaining in the HER XRM system.

For Phase 2, we replaced the Be filter 16 mm in thickness with 0.2 mm in thickness in the HER to reduce small angle scatterings through the Be filter. Such scatterings might result in large smearing effects. Additionally, β_y at the X-ray source point was changed from 7.6 m to 28 m. The Phase 2 measurements show that the smearing effects are reduced to 6.6 µm, indicating that the measurable beam size in the HER can be down to 7 µm. Detailed analyses are ongoing.

Another photon monitor, visible synchrotron radiation monitor (SRM), is also installed one to each main ring [5]. A SRM is essentially an interferometer and simultaneously measures horizontal and vertical beam sizes. After Phase 1, the diamond extraction mirrors located on the upstream of the visible SR lines in the both rings were replaced to gain 200 % large aperture, and baffles were added to reduce the stray light in the visible SR line. At Phase 2, beam size measurements worked well in the HER, but in the LER the SR spot seemed staggering as the beam current increased. We plan to open the mirror chamber for inspection.

The bunch lengths were measured using the streak camera in the both main rings. Figure 7 shows the measured bunch lengths in the HER and the LER. The bunch lengthening behavior in the HER is consistent with the KEKB, because most of the vacuum chambers in the arc and straight sections at SuperKEKB were inherited from KEKB. Though the bunch lengthening in the LER became moderated compared with Phase 1, it still shows unexpected larger lengthening with bunch current.

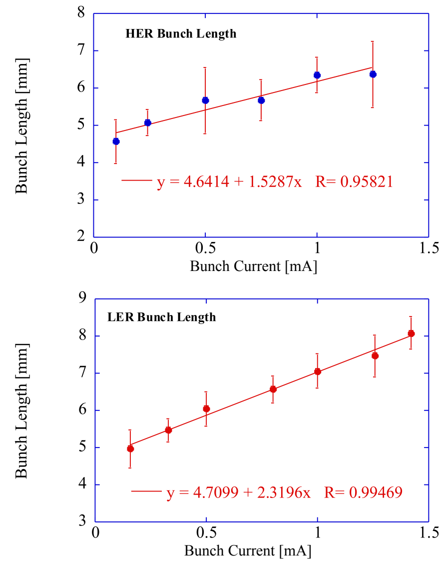

Figure 7: Measured bunch lengths in the HER (upper) and the LER (bottom) as a function of the bunch current.

Bunch Feedback System

Figure 8 shows the block diagram of the bunch-by-bunch feedback systems installed in the HER and LER [6]. The system consists of position detection systems, high speed digital signal processing systems with a base clock of 509 MHz (iGp12 [7]), and wide-band kickers. As we experienced at Phase 1, there was very strong transverse coupled-bunch instabilities in the early stage of Phase 2, which limited the maximum beam currents. By tuning the timing and phase of the transverse feedback systems, we successfully suppressed the coupled-bunch instabilities up to the maximum beam current ~ 800 mA with the minimum bunch separation of 4 ns.

We obtained many transient domain data in the LER during the beam study on electron cloud effects (ECEs). Figure 9 shows an example of growing and damping transients with the 4 ns bunch separation and the beam current of 300 mA in the vertical plane. The distribution of the unstable modes and the growth time show drastic changes compared with those in Phase 1. For example, the fitted growth time constant to the mode 2550 was about 3.9 ms, which is much slower than at Phase 1 (~ 0.8 ms). This tendency is presumably due to the counter measure to suppress ECEs in the drift space. The damping time constant is estimated as < 1 ms, which is consistent with Phase 1.

Concerning longitudinal coupled-bunch instability, we could increase the threshold current from 660 mA (Phase 1) to 800 mA for the nominal collision (3.06 spacing). However, we still encountered the longitudinal coupled-bunch instability in the LER during the ECE study and a challenge to high beam current operation at the very end of Phase 2. The mode and threshold seemed depending on the head position of the vertical collimator nearest to the IP.

ISBN: 978-3-95450-216-5 doi:10.18429/JACoW-eeFACT2018-TUPBB05

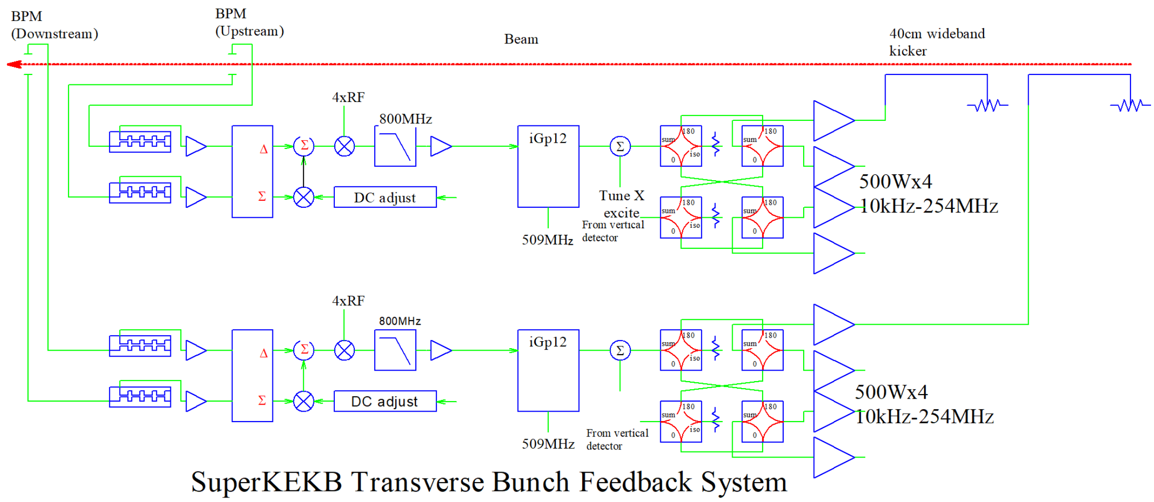

Figure 8: Block diagram of the transverse bunch feedback systems.

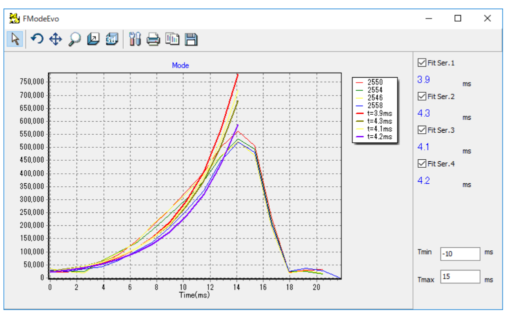

Figure 9: Evolution of the vertical unstable modes with by-2 pattern in the LER at a current of 300 mA.

The longitudinal bunch-by-bunch feedback systems in the LER were not fully functioning at Phase 2 simply due to lack of tuning time. Towards Phase 3 we add two more longitudinal feedback cavities with 1 kW of wide band feedback amplifiers per each cavity. The longitudinal system will be tuned in the early stage of Phase 3.

CONCLUSION

At Phase 2 we could successfully realize the first collision at SuperKEKB and achieve the luminosity 5.55×10^{33} cm^{-2}s^{-1}. It indicates no significant issue found in the nano-beam scheme. All the beam instrumentation systems at SuperKEKB showed excellent performances throughout Phase 2. Particularly newly operated system in the DR since Phase 2 enabled smooth beam commissioning. Further improvements of the instrumentation system are ongoing towards forthcoming Phase 3 physics operation.

ACKNOWLEDGEMENTS

The authors would like to thank the SuperKEKB commissioning group for their help in the operation. This work is partly supported by the US-Japan collaboration in High Energy Physics (R&D for SuperKEKB and the next generation high luminosity colliders).

REFERENCES

[1] P. Raimondi in *2nd LNF Workshop on SuperB*, Frascati, Italy, March 16–18 2006. `http://www.lnf.infn.it/conference/superb06/`

[2] H. Ikeda *et al.* , in Proc. IBIC' 18, Shanghai, China, MOPA02 (2018).

[3] M. Tobiyama *et al.* , in *Proc. IBIC 2013*, MOPF32, 2013, Oxford, GB.; in *Proc. IBIC 2014*, WEPD05, 2014, Monterey, CA, U.S.A.

[4] E. Mulyani and J.W. Flanagan, in *Proc. IBIC 2015*, Melbourne, p.377 (2015); in *Proc. IBIC 2016*, TUPG72, 2016, Barcelona, Spain.

[5] T. Abe *et al.* , Technical Design Report of SuperKEKB, in preparation and to be published as a KEK report. An preliminary version is seen in `https://kds.kek.jp/indico/event/15914/`

[6] M. Tobiyama *et al.* , in *Proc. PASJ2016*, TUOM06, Chiba, Japan.

[7] Dimtel, Inc., `http://www.dimtel.com/`